Influence of Granitic Aggregates from Northeast Brazil on the Alkali-aggregate Reaction

***David de Paiva Gomes Neto*[a,b]*, *Herbet Conceição*[c], *Vinícius Anselmo Carvalho Lisboa*[c],**

***Rodrigo Soares de Santana*[a], *Ledjane Silva Barreto*[a]**

[a]*Postgraduate Program in Materials Science and Engineering – P²CEM,*
Department of Materials Science and Engineering – DCEM, Federal University of Sergipe – UFS,
Av. Marechal Rondon, s/n, Jardim Rosa Elze, CEP 49100-000, São Cristóvão, SE, Brazil
[b]*Federal Institute of Education, Science, and Technology of Sergipe – IFS,*
Av. Eng. Gentil Tavares da Mota, 1166, CEP 49055-260, Aracaju, SE, Brazil
[c]*Department of Geology, Federal University of Sergipe – UFS, São Cristóvão, SE, Brazil*

Received: June 20, 2013; Revised: February 14, 2014

The alkali-aggregate reaction (AAR) in concrete structures is a problem that has concerned engineers and researchers for decades. This reaction occurs when silicates in the aggregates react with the alkalis, forming an expanded gel that can cause cracks in the concrete and reduce its lifespan. The aim of this study was to characterize three coarse granitic aggregates employed in concrete production in northeastern Brazil, correlating petrographic analysis with the kinetics of silica dissolution and the evolution of expansions in mortar bars, assisted by SEM/EDS, XRD, and EDX. The presence of grains showing recrystallization into individual microcrystalline quartz subgrains was associated with faster dissolution of silica and greater expansion in mortar bars. Aggregates showing substantial deformation, such as stretched grains of quartz with strong undulatory extinction, experienced slower dissolution, with reaction and expansion occurring over longer periods that could not be detected using accelerated tests with mortar bars.

Keywords: *granitic aggregates, alkali-aggregate reaction, petrographic analysis, microcrystalline quartz, silica dissolution, mortar bar expansion*

1. Introduction

The alkali-aggregate reaction (AAR) is a phenomenon that has concerned civil engineers and researchers for decades. This reaction has been studied since the early 1940s in order to understand its causes and develop ways to mitigate its effects. Due its complexity, it has attracted the attention of workers in fields as diverse as chemistry, physics, geology, and civil and materials engineering.

There are geographical differences in the options available for mitigation of the AAR, and solutions that are appropriate in one country may not be viable in another. In Brazil, an extremely large country, techniques used in some regions may not be practicable in others. The reasons for these differences include the use of aggregates from a variety of sources, cements with different chemical compositions, different pozzolans and chemical additives, and different environmental exposures.

The AAR occurs when minerals present in the aggregate react with ions (OH^-, Na^+, and K^+) released from hydrated cement paste, forming a hygroscopic gel that expands by uptake of moisture. This causes cracks in concrete that affect its dimensional stability, mechanical properties, and durability. The reaction is initiated by dissolution of silicates present in the aggregates, with attack of hydroxyl ions (OH^-) firstly on silanol groups (Si-OH), and then, in a second stage, on siloxane groups (Si-O-Si), with breaking of the bonds to form dissociated Si-O^- pairs. In both stages, water is released and the cations (Na^+ and K^+) are attracted to counterbalance the negative charges, forming the gel[1,2]. Calcium ions are also involved in the reaction[3,4]. Based on this mechanism, several studies have attempted to associate the potential for dissolution of the silica with the reactivity of different aggregates and silicates[5-9]. Reactive aggregates are usually classified into two groups, according to the kinetics of the reaction. In the first group, comprising vitreous or amorphous minerals such as volcanic glasses and opal, the reactions develop quite rapidly. In the second group, consisting of stressed crystalline minerals such as quartz that has been deformed by tectonic processes, the reactions and expansion are slower[10,11]. Jensen[12] proposed the inclusion of an additional category of highly reactive aggregates, whose members include fine dolomite crystals and expansive clay minerals. Granitic aggregates are included in the group showing slow reactions, where structural defects can occur 10 years after completion of a construction project[12].

Granitic aggregates, composed mainly of quartz, alkaline feldspars, plagioclases, micas, and other secondary minerals, are extensively used in concrete structures worldwide, and can show different responses (in terms of the AAR) in both outdoor structures as well as in laboratory experiments. This is due to the varied textural characteristics

*e-mail: pvgomes@uol.com.br

resulting from thermal and mechanical processing during the geological formation of the minerals, and can hinder direct identification of the principal factors responsible for the reactivity of a given aggregate.

The features associated with the strong deformations suffered by granitic rocks have been suggested to be important indicators of their reactivity. The deformation of quartz, with the development of subgrains and the presence of cryptocrystalline and microcrystalline material, provides important features for evaluation during petrographic analysis[12,13]. Wigum[14], in a study of deformed granitic rocks, found that with the formation of subgrains of quartz, the total grain boundary area and size of grains were the variables that had the greatest influence on the expansion process. Wenk et al.[15] reported that increased deformation and reduced size of the quartz grains led to increased dislocation density, and that this was an important factor affecting the reactivity. However, Hagelia and Fernandes[16] recently suggested that the size of the quartz grains might be less important, and that the dissolution of feldspars and micas contributed to the reactivity. It was shown that structures affected by the AAR presented products of the reaction that were associated with coarse-grained quartz (up to 1500 μm in size, and essentially free of deformation), while granitic mylonites containing microcrystalline quartz and low amounts of mica were found to be innocuous. Tiecher et al.[8] studied the dissolution of three Brazilian aggregates (granite, mylonite, and quartzite) that presented different degrees of deformation. It was found that grains with more deformed textures (quartzite and mylonite), with marked undulatory extinction and deformation bands, dissolved more easily and caused greater expansion in mortar bars, compared to the granite, which had a higher content of recrystallized quartz subgrains. The literature therefore remains inconclusive concerning the influence of quartz subgrains and quartz with smaller dimensions, indicating the need for further studies, both in the field and in the laboratory.

Other relevant characteristics of granitic rocks that have been reported include foliations, cracks, and other alterations of the minerals that enable alkaline solutions to penetrate the interior of the minerals[11]. The presence of mica (especially interstitially) also appears to affect the reactivity of aggregates[15,17].

The combined influences of these factors reflects the complexity of this type of aggregate, indicating the need for studies that take into account the origin of the material, as well as its use at different locations. Studies of granitic aggregates in Brazil have revealed a range of effects in terms of the AAR. In an investigation of aggregates from 26 locations in São Paulo State, Valduga[18] concluded that four out of six coarse granitic aggregates could be considered potentially reactive. Although accelerated tests using mortar bars did not reveal expansions exceeding established limits, the materials presented deformed quartz and undulatory extinction, as well as gels with varied morphologies within the pores of the mortar. Couto et al.[19] studied three granitic aggregates from Goiás State, of which two had massive structures and one had a foliated structure. In all cases, the quartz showed substantial undulatory extinction, although only the foliated granite caused mortar bar expansion that exceeded the established limit. In northeast Brazil, coarse mylonitized aggregates from the Metropolitan Region of Recife were studied by Silva et al.[20]. Reaction damage was identified in samples from the foundations of different buildings in this region, after the collapse of a 12-story building. The greatest expansions in the mortar bars were attributed to the aggregates for which petrographic analysis revealed greater contents of microcrystalline quartz, although altered feldspars and biotite were also detected in the aggregates.

In Sergipe State (northeast Brazil), only one similar study has so far been reported[21]. Three different coarse metamorphic aggregates, collected from concrete manufacturing plants, were subjected to petrographic analysis and mortar bar expansion measurements. Although only two of the aggregates showed alignment of the quartz grains, all three aggregates were found to be potentially reactive. No information was given concerning the presence of quartz subgrains or microcrystalline quartz, so it was not possible to compare the aggregates with those used in the present work.

The AAR is governed by factors common to any heterogeneous chemical reaction with a solid-liquid interface, where the kinetics of the reaction is not only determined by the composition, but also by the surface area, contact surface, form of the particles, and porosity, amongst other factors. The aggregates can present different reaction mechanisms that can only be satisfactorily evaluated using experimental procedures. The investigation of complex systems such as aggregates and alkali-aggregate reactions therefore requires the use of a range of complementary analytical techniques.

Given the uncertainties described above, this study investigated the influence of quartz morphology on the AAR, using three granitic aggregates that are widely employed in reinforced concrete structures in Sergipe State. The work demonstrated that use of a set of complementary techniques is fundamental in understanding the AAR. To this end, petrographic analysis, determination of dissolved silica, and measurement of mortar bar expansion was used, together with scanning electron microscopy (SEM/EDS), energy dispersive X-ray spectroscopy (EDX), and X-ray diffraction analysis (XRD).

2. Material and Methods

The aggregates (samples A, B, and C) were collected directly from distributers. These materials were derived from rocky massifs located in the municipalities of Itabaiana (samples A and B) and Itaporanga D'ajuda (sample C), in central-south Sergipe State.

Compositional analysis and identification of the mineralogical phases in the aggregates was performed by EDX and XRD. The EDX analyses employed a Model EDX 720 spectroscope (Shimadzu). The XRD measurements used a Rigaku diffractometer, operated in scan mode with Cu-Kα radiation (λ = 1.5418 Å), a scan rate of 5°/min, and 2θ between 5° and 80°. These analyses were performed on powdered aggregates that had been passed through a nº. 200 sieve (0.075 mm). For petrographic determination of the textural characteristics of the aggregates, thin sections

were examined using an Opton Model TNP-09T binocular microscope.

Two experimental procedures were used to correlate the results of the composition and texture analyses with the potential reactivity of the aggregates. Measurements of expansion in mortar bars were performed according to the accelerated method described in NBR 15577-5[22], and measurements of dissolved silica were as described in ASTM C 289[23].

Using the accelerated procedure[22], mortar bars (25 x 25 x 285 mm) produced using the aggregates and CP II Z-32 Portland cement were placed in a solution of NaOH (1 mol/L) at 80 °C for 30 days, and the expansions were subsequently measured using a digital dial gauge. An aggregate is considered reactive when bar expansion exceeds a limit value of 0.19% after 30 days, and when petrographic analysis identifies the presence of reactive mineral phases. The measurements were performed in triplicate. The elemental composition of the Portland cement used in the mortar bars was determined by EDX (Table 1). SEM and energy dispersive spectroscopy (EDS) were used for qualitative morphological and elemental analysis of the reaction products in fragments obtained from the mortar bars after the expansion tests. The coupled SEM/EDS analyses were performed with a JEOL JCM-5700 CarryScope instrument operated using a filament voltage of 10 kV. The samples were coated with gold prior to the analyses.

In accordance with the procedure recommended by ASTM C 289 for the determination of dissolved silica[23], 25 g of samples A, B, and C were placed (in triplicate) in PTFE flasks containing 25 ml of NaOH (1 mol/L) and heated at 80 ºC in a water bath. The measurement of dissolved silica was performed using a UV-Vis spectrometer (Libra S12, Biochrom) after reaction of the solutions with hydrochloric acid, oxalic acid, and ammonium molybdate. In addition to the usual 24 hours, dissolution was also measured after 96 and 192 hours. For the purposes of the present study, it was not necessary to use the alkalinity reduction parameter described in the standard procedure. Prior to the dissolved silica assays, the aggregate samples were pulverized and then sieved. The particles selected were those that passed through a nº. 50 (0.3 mm) sieve and those that were retained on a nº. 100 (0.15 mm) sieve.

Table 1. Elemental and compositional analyses of the samples and cement using EDX analysis.

Oxides	Sample A	Sample B	Sample C	Cement
SiO_2	67.13	70.34	66.53	22.69
Al_2O_3	17.29	17.24	17.28	5.27
K_2O	3.85	3.89	4.27	1.32
Na_2O	3.21	3.51	2.12	-
Fe_2O_3	3.05	1.87	3.72	3.1
CaO	2.63	1.77	3.05	61.64
MgO	1.69	0.68	1.82	1.15
SO_2	0.55	0.24	0.3	4.36
TiO_2	0.31	0.21	0.59	0.25

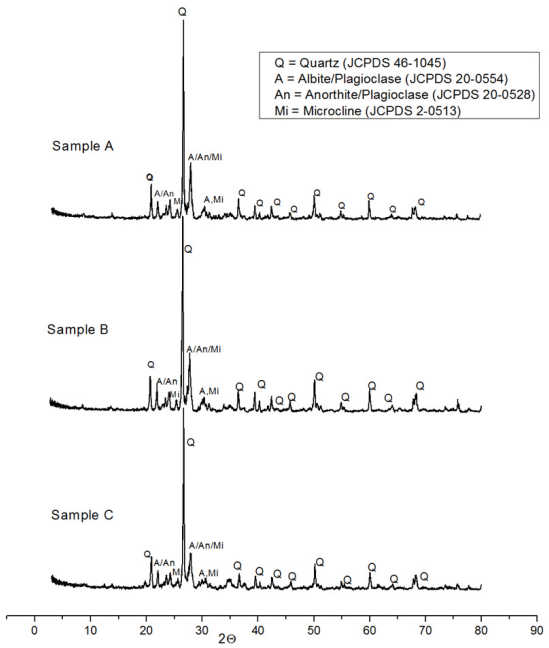

Figure 1. Results of XRD analyses of samples A, B, and C.

3. Results

The elemental and compositional analyses (Table 1) showed that the three aggregates contained around 70% Si, 17% Al, and smaller amounts of Na, K, Ca, Fe, and Mg. The XRD results (Figure 1) were similar for the three samples, with main peaks corresponding to quartz (SiO_2, JCPDS 46-1045), microcline (potassium feldspar, $KAlSi_3O_8$, JCPDS 2-0513), and plagioclase ($NaAlSi_3O_8$, JCPDS 20-0554, and $CaAl_2Si_2O_8$, JCPDS 20-0528). However, although these results indicated that the aggregates had similar chemical compositions, textural evaluation using optical microscopy revealed significant differences, especially in the case of sample C.

Optical microscopy images were acquired for thin sections, using crossed nicols and plane-polarized light. The main characteristics are provided in Table 2. Figure 2 shows an overview of the section of sample A. The observed alignment was caused by tectonic anisotropism (mylonitic foliation). The inequigranular structure resulted from the presence of feldspar phenoclasts and a matrix that occupied 38% of the volume of the sample. The minerals were of fine granulation, with grains that varied between 0.01 and 4.5 mm in size. Most grains were within the 0.8-1.4 mm size range. Quartz, which accounted for 31% of the sample, was present as stretched anhedral grains (ribbon quartz, as shown in Figure 3), with strong undulatory extinction and sutured boundaries, and dimensions of between 0.05 and 1.6 mm (although fewer than 10% of the grains were smaller than 150 μm). The process of mylonitization resulted in recrystallization of the quartz grains, with some subgrains already formed and others in the process of formation (Figure 3). The most abundant phenoclasts consisted of microcline (30.6%), sometimes with sigmoidal and fractured features. These grains were anhedral, with dimensions of

Table 2. Characteristics of the aggregates.

Characteristics	Sample A	Sample B	Sample C
Nature	Meta-igneous	Meta-igneous	Metamorphic
Name	Mylonitized hornblende granodiorite	Granodiorite/ mylonitized granite	Granoblastite
Color	Greenish-gray	Gray	Reddish
Structure	Anisotropic and inequigranular	Anisotropic and inequigranular	Isotropic and equigranular
Grain	Fine-grained	Fine-grained	Fine-grained

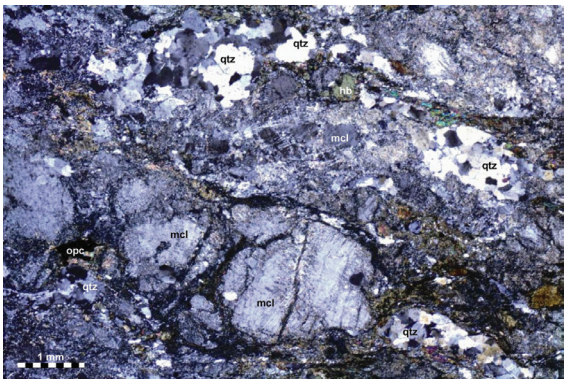

Figure 2. Overview of the section of sample A using crossed nicols, showing alignment of the grains, the tectonic matrix, inequigranular structure, and fractured microcline (qtz = quartz; hb = green hornblende; mcl = microcline; opc = opaque minerals).

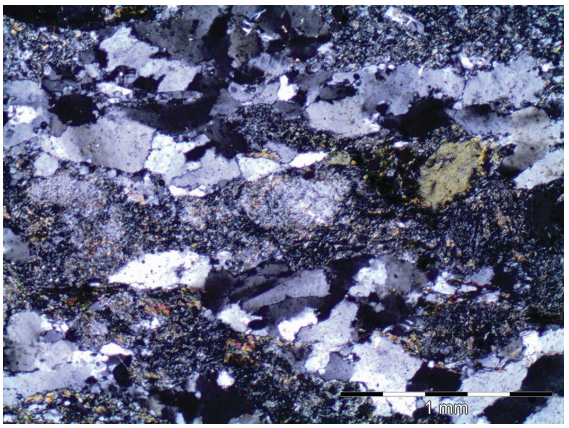

Figure 3. Stretched grains of quartz (ribbon quartz) with formation of subgrains, surrounded by a fine-grained matrix.

between 0.01 and 4.5 mm, and there was considerable evidence of white mica. The plagioclase grains (34.4%) were also anhedral, with dimensions between 0.01 and 0.8 mm, and in some cases, there was evidence of alteration resulting in formation of a mixture of epidote, white mica, and carbonate. Less abundant components included green hornblende (3.1%) and opaque minerals (0.9%). Carbonate represented less than 0.1% of the sample.

An overview of the section of sample B is provided in Figure 4. This sample also showed alignment caused by tectonic anisotropism (mylonitic foliation), albeit to a lesser extent than observed for sample A, and was inequigranular,

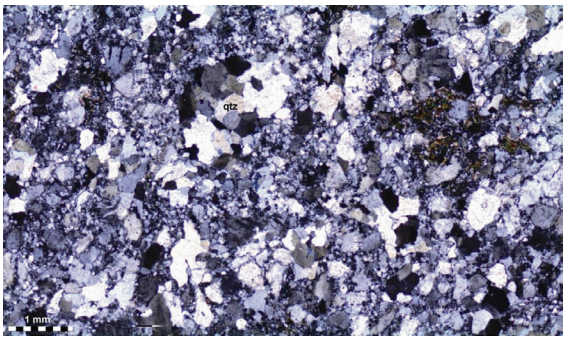

Figure 4. Overview of the section of sample B, showing low intensity mylonitic foliation, reduced tectonic matrix, inequigranular structure, and reduced formation of quartz subgrains. (qtz = quartz)

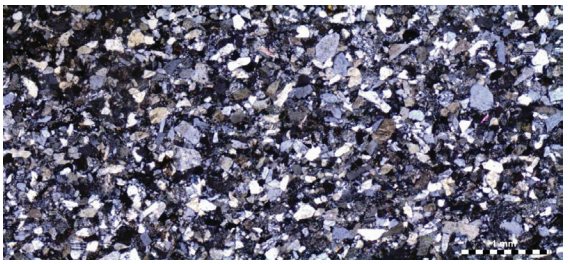

Figure 5. Overview of the section of sample C, showing the equigranular structure, absence of a tectonic matrix, and no grain alignment.

with fine granulation and a tectonic matrix that occupied 25-30% of the total volume. The quartz (28.8%) consisted of anhedral grains with sutured boundaries and dimensions varying between 0.01 and 0.3 mm. Fewer than 10% of the grains were smaller than 150 µm, and undulatory extinction intensity was moderate to strong. In contrast to sample A, the formation of stretched recrystallized phenoclasts was rare. The microcline (35.8%) was anhedral, with dimensions between 0.08 and 0.4 mm, and many of the grains were altered to white mica. The plagioclases (30.4%) consisted of grains that were anhedral, subhedral, and (rarely) euhedral, with dimensions between 0.01 and 1.8 mm. These grains showed a high degree of saussuritic alteration. Brown biotite (2.8%) was a minor component, with grain sizes between 0.01 and 0.2 mm, and with some of the grains showing alteration to chlorite. Other minor components were hornblende (1.4%) and opaque minerals (0.6%), while carbonate accounted for less than 0.1% of the sample.

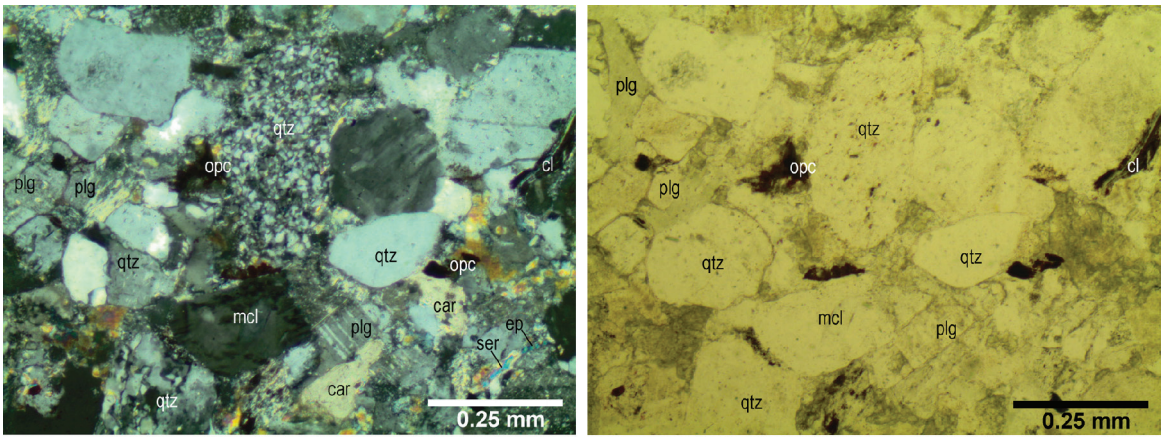

(a) (b)

Figure 6. View of microcrystalline quartz subgrains formed by recrystallization, (a) observed using crossed nicols, (b) observed using plane-polarized light. (qtz = quartz, plg = plagioclase, mcl = microcline, car = carbonate, ser = sericite, cl = chlorite, opc = opaque minerals, ep = epidote).

The textural characteristics of sample C were distinct from those of the other samples. In this case, there was no alignment of the grains, and the tectonic matrix was absent (Figure 5). The quartz (20.5%) was present as anhedral grains with dimensions varying between 0.02 and 0.3 mm (around 20% of the grains were smaller than 150 µm), and undulatory extinction was mild. There were no typical signs of deformation (in contrast to sample A), although many of the grains showed recrystallization into individual microcrystalline subgrains (smaller than 20 µm), probably due to thermal metamorphism (Figure 6). The microcline (35.4%) consisted of anhedral grains sized between 0.01 and 2 mm, with grains of around 0.8 mm predominating, many of which were altered to white mica. The plagioclases were present as anhedral and subhedral grains sized between 0.01 and 0.8 mm. There was substantial saussuritic alteration, and epidote grains of up to 0.5 mm in size. The micas were present in the form of interstitial brown biotite (1.8%), with grain sizes smaller than 0.1 mm and strong alteration to chlorite (Figure 7), as well as white mica (less than 0.1%) in the form of flakes sized between 0.03 and 0.2 mm, which is generally associated with microcline. Opaque minerals and carbonate accounted for less than 0.1% of the sample.

Investigation of the correlation between the texture of the aggregates and the AAR involved the determination of dissolved silica and measurements of expansion in mortar bars. Identification of the reaction products was performed using SEM/EDS.

The results of the determination of dissolved silica after heating in a solution of NaOH (Figure 8) revealed that sample C showed fastest dissolution up to 96 hours of exposure (2.5 times greater than for the other samples), with attainment of equilibrium within 192 hours of treatment. Dissolution of samples A and B only reached levels similar to that of sample C after 192 hours, indicating that the reaction kinetics of sample C was different, compared to the other samples. This behavior was coherent with the mortar

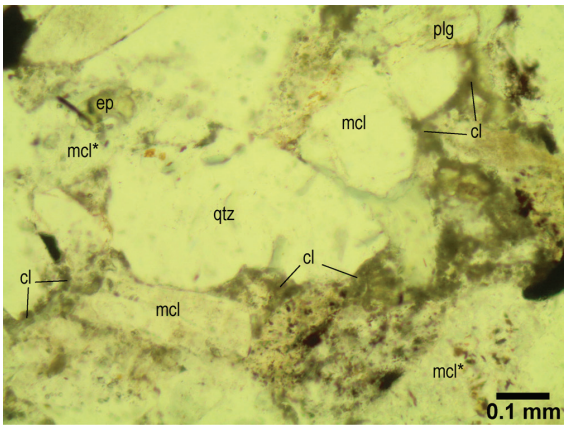

Figure 7. Interstitial chlorite observed using plane-polarized light (cl = chlorite, mcl* = altered microcline, ep = epidote, qtz = quartz, plg = plagioclase).

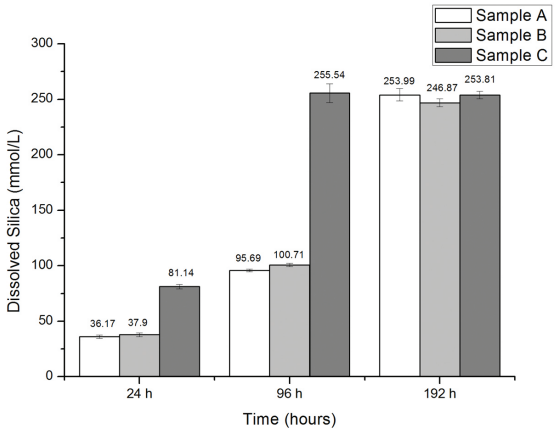

Figure 8. Concentrations of dissolved silica after different times.

bar expansion results (Figure 9). Bars made with sample C showed expansions of around 0.27% after 30 days, while bars made with samples A and B showed average expansions of 0.18 and 0.10%, respectively.

These results were confirmed by morphological analysis of the reaction products formed in the bars after expansion. The SEM images and semi-quantitative chemical analysis by EDS (Figure 10) revealed the formation of AAR products in the pores of a bar fragment produced with sample C, with morphology and composition (in terms of Si, Na, K, and Ca) in accordance with previous work[6,24]. Images of the interior of the mortar bars produced with samples A and B mainly showed pores that were empty (Figure 11), or that were filled with products of the hydration of cement, such as hexagonal crystals of portlandite ($Ca(OH)_2$) (Figure 12).

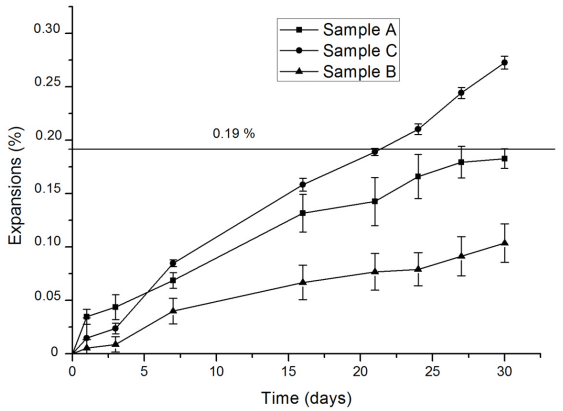

Figure 9. Mortar bar expansions.

4. Discussion

The results of the mortar bar expansion measurements were in agreement with the analyses of dissolved silica and indicated the greater propensity of sample C to develop the AAR. In the case of the other samples, dissolution of sample B was slightly greater than that of sample A in the first 96 hours, although this was reversed after 192 hours of treatment. The SEM/EDS analyses revealed that the interior of the bars containing sample C contained fissured pores filled with products of the reaction, further supporting the hypothesis that expansion in these bars was related to the AAR.

The XRD and EDX analyses showed that the differences in expansion behavior and silica dissolution could not be attributed to the chemical and mineralogical characteristics of the aggregates. However, the petrographic analyses indicated that the differences could be explained by the different textural properties. In sample C, the presence of subgrains of microcrystalline quartz smaller than 20 μm (Figure 6), which have been described as being reactive to highly reactive[13], resulting from the process

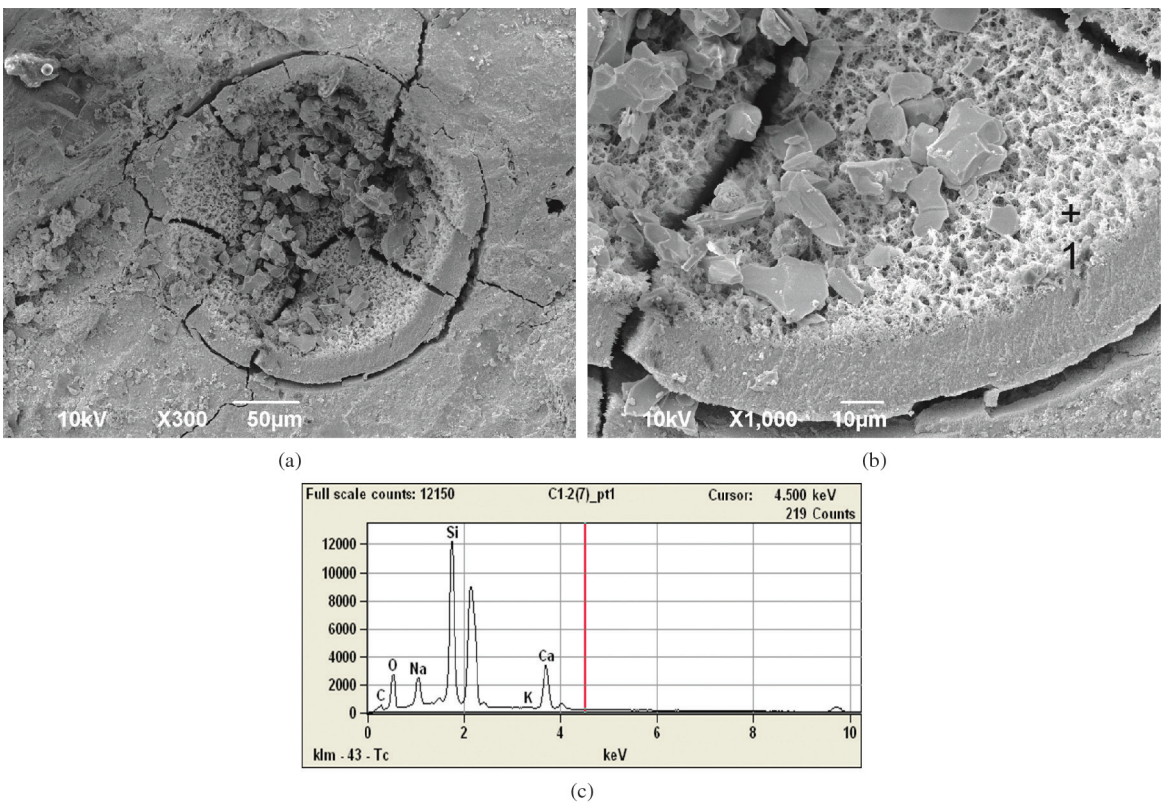

Figure 10. SEM image of (a) a pore filled with AAR products in a fragment of a bar made with sample C, (b) a detail of AAR products, and (c) EDS analysis of the AAR products.

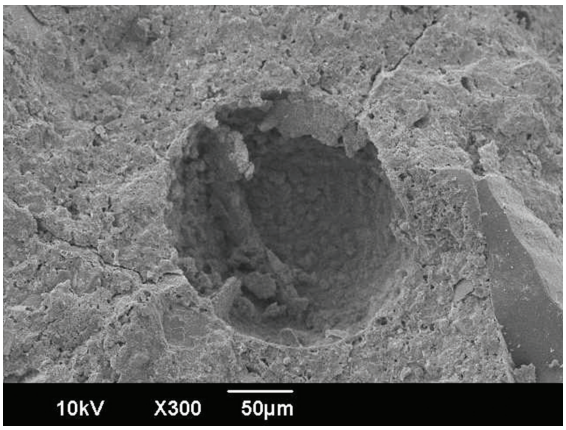

Figure 11. Empty pore in the interior of a mortar bar made using sample A.

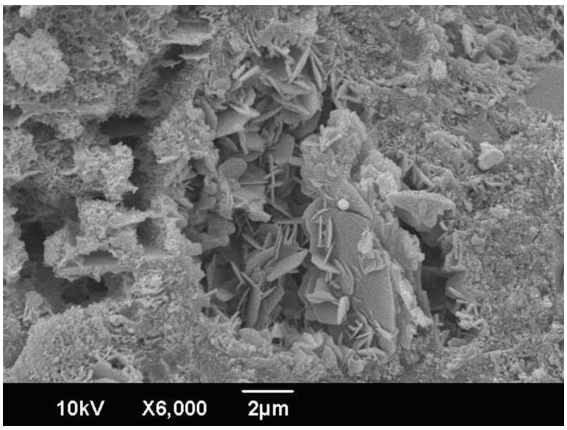

Figure 12. Pore filled with portlandite in the interior of a mortar bar made using sample B.

of recrystallization of larger grains, could explain the fast dissolution of silica and greater expansion in the mortar bars. The smaller size of the quartz subgrains in sample C implies that this material had a greater surface area and an increased number of grain boundaries, compared to samples A and B, favoring faster reaction at the solid-liquid interface, in agreement with the kinetics of a heterogeneous chemical reaction.

In addition, the interstitial brown biotite (altered to chlorite) in sample C could have contributed to rapid silica dissolution, despite only accounting for 1.8% of the sample volume. The presence of interstitial mica has recently been reported in the aggregate of a structure severely affected by the AAR[17].

The kinetic behavior observed for samples A and B was similar. The reactive components dissolved more slowly, which meant that the expansion reactions were delayed and no pronounced effects were observed during the 30 days of the mortar bar assays. This was in agreement with classification of the deformed aggregates of these samples into the category of slow reaction aggregates[10-12]. Nonetheless, other studies have shown that deformed aggregates can show greater effects of the reaction after periods longer than 30 days[25,26].

5. Conclusions

The techniques employed here showed that rapid rates of silica dissolution and expansion in mortar bars containing sample C (granoblastite) were directly related to the presence of individual microcrystalline quartz subgrains derived from the recrystallization of larger grains. The presence of interstitial biotite could also have contributed to the fast dissolution of silica in sample C. In contrast, in the case of samples A and B (granodiorites), the main factors affecting the kinetics were substantial deformations, such as stretched quartz grains with strong undulatory extinction, which contributed to slower dissolution, with reaction and expansion over longer periods that could not be detected using accelerated tests with mortar bars.

References

1. Dent Glasser LS and Kataoka N. The chemistry of alkali-aggregate reaction. *Cement and Concrete Research*. 1981; 11:1-9. http://dx.doi.org/10.1016/0008-8846(81)90003-X
2. Kurtis KE and Monteiro PJM. Chemical additives to control expansion of alkali-silica reaction gel: proposed mechanisms of control. *Journal of Materials Science*. 2003; 38:2027-2036. http://dx.doi.org/10.1023/A:1023549824201
3. Dent Glasser LS and Kataoka N. On the role of calcium in the alkali-aggregate reaction. *Cement and Concrete Research*. 1982; 12:321-331. http://dx.doi.org/10.1016/0008-8846(82)90080-1
4. Chatterji S, Jensen AD, Thaulow N and Christensen P. Studies of alkali-silica reaction. Part 3. *Cement and Concrete Research*. 1986; 16:246-254. http://dx.doi.org/10.1016/0008-8846(86)90141-9
5. Bulteel D, Garcia-Diaz E, Vernet C and Zanni H. Alkali-silica reaction: A method to quantify the reaction degree. *Cement and Concrete Research*. 2002; 32:1199-1206. http://dx.doi.org/10.1016/S0008-8846(02)00759-7
6. Leemann A and Holzer L. Alkali-aggregate reaction – identifying reactive silicates in complex aggregates by ESEM observation of dissolution features. *Cement and Concrete Composites*. 2005; 27:796-801. http://dx.doi.org/10.1016/j.cemconcomp.2005.03.007
7. Multon S, Cyr M, Sellier A, Leklou N and Petit L. Coupled effects of aggregate size and alkali content on ASR expansion. *Cement and Concrete Research*. 2008; 38:350-359. http://dx.doi.org/10.1016/j.cemconres.2007.09.013
8. Tiecher F, Rolim PH, Hasparik NP, Dal Molin DCC, Gomes MEB and Glieze P. Reactivity study of Brazilian aggregates through silica dissolution analysis. In: *Proceedings of the 14th Conference on Alkali-Aggregate Reaction in Concrete;* 2012; Austin. 10 p.
9. Gao XX, Cyr M, Multon S and Sellier A. A comparison of methods for chemical assessment of reactive silica in concrete aggregates by selective dissolution. *Cement and Concrete*

Composites. 2013; 37:82-94. http://dx.doi.org/10.1016/j.cemconcomp.2012.12.002

10. Associação Brasileira de Norma Técnicas - ABNT. *NBR 15577-1*: Agregados – Reatividade Álcali-Agregado. Parte 1: Guia para avaliação da reatividade potencial e medidas preventivas para uso de agregados em concreto. Rio de Janeiro: ABNT; 2008. 11 p. (in Portuguese).
11. Ponce JM and Batic OR. Different manifestations of the alkali-silica reaction in concrete according to the reaction kinetics of reactive aggregate. *Cement and Concrete Research*. 2006; 36:1148-1156. http://dx.doi.org/10.1016/j.cemconres.2005.12.022
12. Jensen V. Reclassification of alkali aggregate reaction. In: *Proceedings of the 14th Conference on Alkali-Aggregate Reaction in Concrete;* 2012; Austin. 10 p.
13. Alaejos P and Lanza V. Influence of equivalent reactive quartz content on expansion due to alkali silica reaction. *Cement and Concrete Research*. 2012; 42:99-104. http://dx.doi.org/10.1016/j.cemconres.2011.08.006
14. Wigum BJ. Examination of microstructural features of Norwegian cataclastic rocks and their use for predicting alkali-reactivity in concrete. *Engineering Geology*. 1995; 40:195-214. http://dx.doi.org/10.1016/0013-7952(95)00044-5
15. Wenk H-R, Monteiro PJM and Shomglin K. Relationship between aggregate microstructure and mortar expansion. A case study of deformed granitic rocks from the Santa Rosa mylonite zone. *Journal of Materials Science*. 2008; 43:1278-1285. http://dx.doi.org/10.1007/s10853-007-2175-8
16. Hagelia P and Fernandes I. On the AAR susceptibility of granitic and quartzitic aggregates in view of petrographic characteristics and accelerated testing. In: *Proceedings of the 14th Conference on Alkali-Aggregate Reaction in Concrete;* 2012; Austin. 10 p.
17. Fernandes I. Composition of alkali-silica reaction products at different locations within concrete structures. *Materials Characterization*. 2009; 60:655-668. http://dx.doi.org/10.1016/j.matchar.2009.01.011
18. Valduga L. *Reação álcali-agregado: mapeamento de agregados reativos do estado de São Paulo*. [Thesis]. Campinas: Universidade Estadual de Campinas. (in Portuguese).
19. Couto T, Casarek H, Hasparik NP and Monteiro P. A potencialidade reativa dos agregados do estado de Goiás. In: *Anais do 50º Congresso Brasileiro do Concreto;* 2008; Salvador. 20 p. (in Portuguese).
20. Silva FCS, Monteiro ECB, Gusmão AD and Silva PN. Análise dos limites de expansão de normas do método acelerado das barras. In: *Anais do 51º Congresso Brasileiro do Concreto;* 2009; Curitiba. 16 p. (in Portuguese).
21. Cardoso AS, Hasparik NP and Dórea SCL. Reação álcali-agregado: potencialidade reativa dos agregados utilizados em concretos no estado de Sergipe. In: *Anais do 51º Congresso Brasileiro do Concreto;* 2009; Curitiba. 20 p. (in Portuguese).
22. Associação Brasileira de Norma Técnicas - ABNT. *NBR 15577-5*: Agregados – Reatividade Álcali-Agregado. Parte 5: Determinação da Mitigação da Expansão em Barras de Argamassa pelo Método Acelerado. ABNT; 2008. (in Portuguese).
23. American Society for Testing and Materials – ASTM. *C 289*: Standard Test Method for Potential Alkali-Silica Reactivity of Aggregates (Chemical Method). ASTM; 2007.
24. Puertas F, Palacios M, Maroto AG and Vásquez T. Alkali-aggregate behavior of alkali-activated slag mortars: effect of aggregate type. *Cement and Concrete Composites*. 2009; 31:277-284. http://dx.doi.org/10.1016/j.cemconcomp.2009.02.008
25. Tiecher F, Dal Molin DCC, Gomes MEB, Rolim PH and Hasparik NP. Análise da potencialidade de desenvolvimento da reação álcali-agregado em função da dissolução de sílica dos agregados. In: *Anais do 52º Congresso Brasileiro do Concreto;* 2010; Fortaleza. 14 p. (in Portuguese).
26. Hasparik NP, Monteiro PJM and Dal Molin DCC. Avaliação em laboratório do potencial reativo para a RAA do agregado quartzito procedente da UHE Furnas. In: *Anais do 50º Congresso Brasileiro do Concreto;* 2008; Salvador. 20 p. (in Portuguese).